Applied Surface Science 290 (2014) 1–5

Contents lists available at ScienceDirect

Applied Surface Science

journal homepage: www.elsevier.com/locate/apsusc

Laser-assisted implantation of gold nanoparticles, formed under surface plasmon-polariton resonant conditions in polymer layer

L. Fedorenko*, I. Matyash, Z. Kazantseva, S. Rudenko, Ya. Kolomiychenko

V.E. Lashkaryov Institute of Semiconductor Physics, NAS of Ukraine, Ukraine

ARTICLE INFO

Article history:
Received 1 March 2013
Received in revised form 4 October 2013
Accepted 21 October 2013
Available online 21 November 2013

PACS:
81.16.Mk
81.07.Bc
79.20.Ds

Keywords:
Laser-assisted microablation
Surface plasmon-polariton resonance
Nanoparticles implantation
Polymer film

ABSTRACT

Morphological and optical properties of a polymer film/glass system with laser-implanted Au nanofragments were studied. The polymer films (formvar) were deposited on glass plates by the Langmuir–Blodgett method. The fragmentation of continuous Au films was carried out by a Q-switched YAG:Nd^{3+} laser ($\lambda = 532$ μm, $t_p = 10$ ns) at the condition of the surface plasmon-polariton resonance (SPR) and subsequent ballistic transport of Au nanoparticles (NPs) through the air gap and fixation in the polymer film. It is shown that the average size and concentration of the implanted NPs are significantly influenced by the SPR. They were ranged from 40 nm and 6.5×10^9 cm^{-2} up to 350 nm and 5×10^7 cm^{-2} at the resonant and nonresonant cases, respectively. Possible mechanisms of decomposition of the Au film fragments are discussed within the framework of a thermal model.

1. Introduction

Recent developments of nanoplasmonics open new opportunities to improve the characteristics of sensor devices by increasing the sensitivity of the surface layer. Currently, the laser-assisted methods based on the plasmon resonance effect [1,2] allow to control both size and shape of Au and Ag during their formation by irradiation of colloid and gel solutions which already contain the metal particles by high power laser pulses and for the completion of the nano fragmentation process takes time for several hours [3].

In our previous works [4,5] the possibility of laser-assisted nanofragmentation of Au films under the SPR condition at the laser excitation close to the melting threshold was shown. The continuous Au film deposited on a glass substrate served as a source of Au NPs, which were obtained using laser fluence (LF) at a level that exceed the microablation threshold at the SPR conditions. The Au NPs were transferred to the polymer film through the thin air gap.

2. Experimental

The second harmonic of YAG:Nd^{3+} laser 1 ($\lambda = 0.532$ μm, $t_p = 10$ ns) was used for the plasmon-polariton laser fragmentation of the Au film 2, Fig. 1. The same laser pulse was used to transfer of Au NPs through the air gap ($h_{air} \approx 50$ μm, see insertion) and their incorporation into the polymer film 3 with a thickness $d_f = 60$ nm on the glass substrate 4. The source film was deposited by vacuum evaporation on the glass plate 5 previously covered by a thin Cr sub-layer with thickness of ~2 nm to improve of Au adhesion. This source plate complements the glass segment 6 to the semi-cylinder using an immersion layer 7 (glycerin) to implement Kretchman configuration of irradiation. Both were made of flint glass.

Optical parameters of the structured polymer films were determined experimentally by the method of modulation of the polarized coherent radiation under an internal reflection from the system glass/polymer film/air (also in Kretchman geometry), Fig. 2. The photo-elastic polarization modulator PEM is the dynamic phase plate which mode and azimuth position are chosen such that the glass semi-cylinder is illuminated alternately by *p*- and *s*-polarized He–Ne laser radiation. The reflected radiation was recorded by a photodetector PD. Since the reflection coefficients of *p*-polarized R_P and *s*-polarized waves R_S are various, the measured by a selective voltmeter signal ΔI at a modulation frequency is proportional to the difference $\Delta I \sim \Delta R = R_S - R_P$. The linear polarizer *G* in the front of a photodetector results in modulation of the intensity of that polarization with respect to which the polarizer is oriented to transmission. The measurement technique is described in details previously [6]. Here we just note that ΔR is directly measured physical quantity, but not the result of mathematical subtraction of R_S and R_P.

* Corresponding author. Tel.: +380 440963639245; fax: +380 445258342.
E-mail addresses: l170843@voliacable.com, lfedor@isp.kiev.ua (L. Fedorenko).

0169-4332/$ – see front matter © 2013 Elsevier B.V. All rights reserved.
http://dx.doi.org/10.1016/j.apsusc.2013.10.123

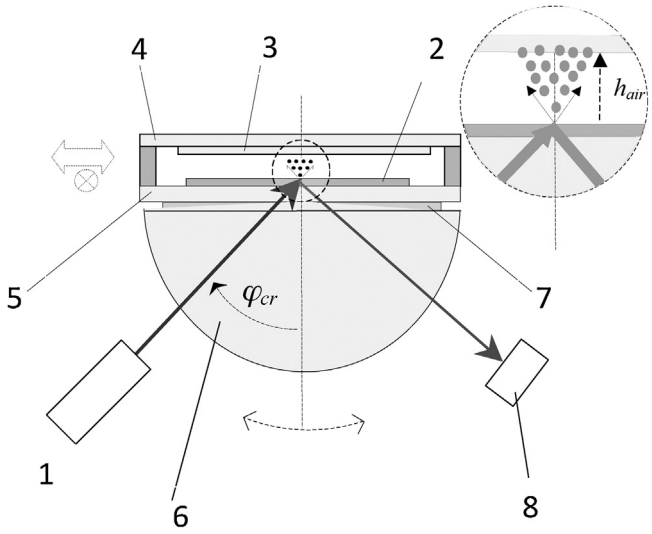

Fig. 1. Experimental setting of SPR:1, YAG:Nd^{3+} laser; 2, Au film; 3, polymer layer (formvar); 4, protective glass plate; 5, glass plate; 6, semicylindrical prism; 7, immersion layer; 8, photodiode.

3. Results

Typical AFM images of the polymer film surface after implantation of Au NPs are shown in Fig. 3a with (a) and without (b and c) SPR conditions ($R = R_{min}$ and $R \neq R_{min}$, respectively). It is seen that in the first case the gold NPs with the circular-shaped cross section and the average size of $\langle \delta \rangle = 40$ nm and surface concentration $\langle n \rangle = 5 \times 10^9$ cm^{-2} are obtained, while in the second case gold particles have arbitrary cross-section. Also, they have larger dimension and lower concentration (typical values are $\langle \delta \rangle = 350$ nm and $\langle n \rangle = 6.5 \times 10^7$ cm^{-2}). The characteristics of the reflection R_S, R_P and ΔR at the scanning wavelength $\lambda = 630$ nm for a representative sample obtained at the SPR condition are shown in Fig. 4 in relative units. Shown in Fig. 5 are experimental angular dependences of the polarization difference ΔR, obtained by reflection from the regions of the formvar film implanted by Au NPs in the case of the SPR, without the SPR, as well as, from the pure surface of the glass semi-cylinder without the Au film.

The calculated three-dimensional diagram of the polarization difference as a function of the film thickness and the incidence angle of the scanning beam is presented in Fig. 6. In spite of the absence of criterions of the resonant interaction of radiation with the film, the range of angles which are more than the critical one is of the most interest. It should be noted that the range of thickness d in Fig. 6 is very small, $d = 0 \div 3.5$ nm. This is the only range in which the polarization difference is positive at angles more than the critical angle and it shows the nonresonance interaction.

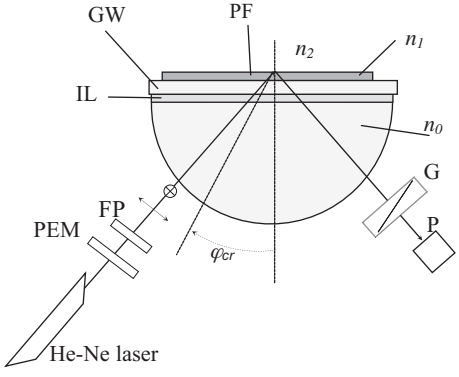

Fig. 2. Optical scheme of the polarization modulation method. PF, polymer film; PEM, photoelastic polarization modulator; FP, phase plate; IL, immersion layer; GW, glass wafer; φ_{cr}, critical angle of total internal reflection; n_0, n_1, n_2, refractive indexes of glass, studied film and air, respectively.

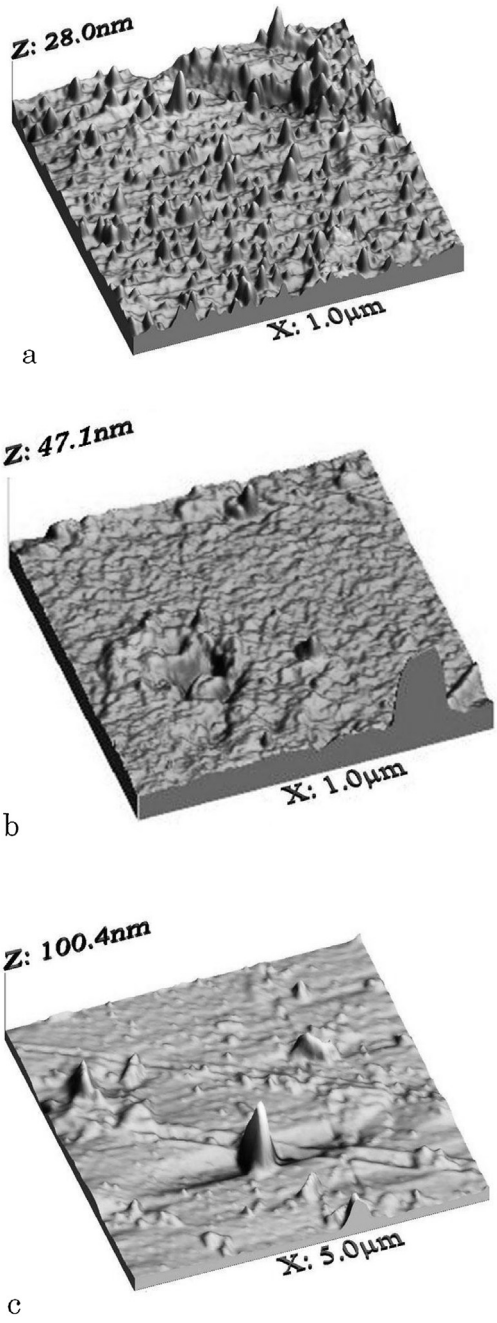

Fig. 3. AFM images of the polymer film surface after YAG:Nd^{3+} laser irradiation ($\lambda = 0.532$ μm, $t_p = 10$ ns) (a) under ($R = R_{min}$), and (b and c) without SPR ($R \neq R_{min}$) condition.

4. Discussion

To understand experimental results a model of transmission and reflection is considered, using the formalism of the Fresnel equation [7]. The intensity and polarization of testing laser beam is changed during the passage of each layer and reflection on the boundaries, Fig. 2. The product of matrices that describe these changes in the sequence of light passing provides a state of polarization in the final form (described in detail in [5]). In this simulation, three variables